DISLOCATION MODELLING OF SHORT FATIGUE CRACK GROWTH THROUGH ALTERNATING SLIP

P. Hansson, S. Melin
Division of Mechanics
Lund Institute of Technology, Box 118, SE-22100 LUND
Per.Hansson@solid.lth.se

Abstract

The mechanisms behind the growth of a short edge crack, located within one grain, have been investigated in bcc iron under cyclic loading conditions. The crack grows by single shear along preferred slip planes due to emission and annihilation of discrete dislocations, leading to a zigzag crack shape. The model is a combination of a discrete dislocation formulation and a boundary element approach. All external boundaries including the crack are modelled by dislocation dipole elements and the local plasticity is modelled by discrete dislocations, allowed to move along preferred slip planes. An in penetrable grain boundary restricts the spread of plasticity. The model makes it possible to study the crack growth path, the crack shape and the development of the plastic zone in detail. It is shown that the grain orientation determines the precise crack path for a fixed slip system.

Introduction

For short cracks, when the plastic zone is significant in comparison with the crack length, linear elastic fracture mechanics can not be used and the well established methods to estimate the crack growth rate for a long crack, Paris' law [1], can not be used. The growth of short cracks is driven by shear and is dominated by local plasticity. The growth is also strongly influenced by the microstructure of the material, grain orientation and grain size. This has been shown by numerous experimental investigations of events taking place during fatigue crack growth. Andersson and Persson [2], Suresh [3], Jono *et al.* [4] and Zhang [5] have performed microscopic studies showing that a fatigue crack grows by single shear along preferred slip planes. In order to be able to improve fatigue life estimates, especially for materials that spend a large portion of the total life before entering the Paris' region, the growth of short fatigue cracks must be further understood.

For low growth rates, it is important to account for the discrete dislocations within the material. Studies taking this into account have been performed by Riemelmoser *et al.* [6] and Riemelmoser and Pippan [7]. They have modelled the interaction between a long mode I crack subjected to cyclic loading and individual dislocations in the material. Bjerkén and Melin [8,9] have studied microstructurally short mode I fatigue cracks, where crack growth occurs due to dislocation emission and annihilation at the crack tip. The model is entirely based on a dislocation formulation. A similar method has been used by Uematsu *et al* [10]. to study the crack deflection behaviour in body centred cubic (bcc) iron. The stresses and displacements were calculated by superposition of two elastic fields, one describing the discrete dislocations and the other the crack itself.

In this study a combination of a discrete dislocation formulation and a boundary element approach is used. The external boundary, including the crack itself, is modelled by dislocation dipole elements as suggested in [8], and the plasticity is modelled by discrete

dislocations situated along certain preferred slip planes. Here the method is used to study the quasi-static growth of a short edge crack. The crack is situated within one grain in a bcc material and is extending by single shear due to emission and annihilation of dislocations when subjected to cyclic loading under plane strain conditions.

Problem formulation

The quasi-static growth of a short edge crack located within one grain and subjected to fatigue loading has been investigated under plane strain conditions. The original crack is inclined an angle α, coinciding with a preferred slip direction, to the normal of the free edge and an external load σ_{yy}^{∞} is applied parallel to the edge, cf. Fig. 1. The applied load is varied between a maximum value, $\sigma_{yy\,max}^{\infty}$, and a minimum value, $\sigma_{yy\,min}^{\infty}$. It is assumed that the crack grows through single shear along preferred slip planes, indicated by dashed lines in Fig. 1. The slip planes within the grain are separated an angle β, depending on the orientation of the grain and the crystal lattice of the material. An in penetrable grain boundary is present at a certain distance in front of the original crack tip and is parallel to the free edge.

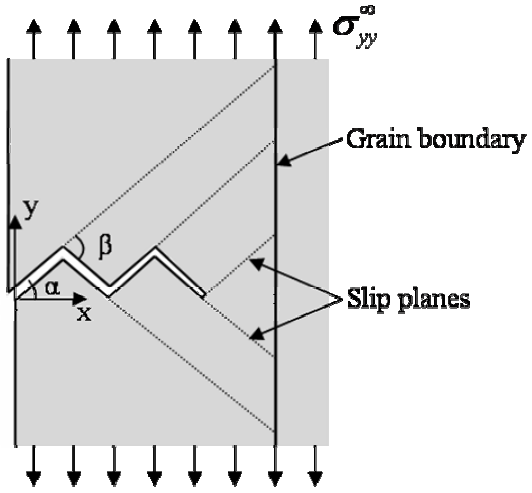

FIGURE 1. Geometry of the short edge crack.

At each instant the resolved shear stress is calculated along all slip planes where dislocations already exist or can be expected to nucleate, i.e. along the dashed lines in Fig. 1. When the resolved shear stress exceeds the nucleation stress τ_{nuc} at a certain distance r_{nuc} from the crack tip or from a corner point of the crack, an edge dislocation pair will nucleate at r_{nuc}. A dislocation pair consists of two dislocations of equal size but of opposite direction. When nucleated the dislocation with the positive Burgers vector moves along a slip plane inwards in the material as long as the resolved shear stress at the point were the dislocation is situated exceeds the critical resolved shear stress τ_{crit}. τ_{crit} is the lattice resistance to slip along the preferred slip plane in the material and is considered a material parameter. The dislocation with the negative Burgers vector annihilates at the crack surface and causes either a slip between the crack surfaces or the crack to open, depending on which slip plane it was nucleated on. The crack advances during the unloading part of the cycle as dislocations with positive Burgers vectors get close enough to the crack to be annihilated, assuming that no healing of the crack surface occurs.

The characteristics of the material in this study are those of pure iron with a bcc crystal structure. In a bcc material slip occurs along close packed $\langle 111 \rangle$ directions, cf. eg. Hull and Bacon [11]. In this study it is assumed that slip occurs in the close-packet (110) plane in the [-1 1 1] and [1 -1 1] directions. This results in two possible slip systems in 2-D, with two alternative angles β between the slip planes, β = 70.6° or β = 109.4°.

The material is bcc-Fe with shear modulus μ = 80 GPa and Poisson's ratio ν = 0.3, cf. eg. Askeland [12]. The size of the Burgers vector b = 0.25 nm and the critical resolved shear stress is τ_{crit} = 40 MPa [8].

Modelling of the external boundary

The external boundary, defined as the free edge together with the crack surfaces, is modelled by dislocation dipole elements in a boundary element approach, cf. [8]. Only plane problems will be addressed and therefore only edge dislocations are needed in the formulation. A dislocation dipole element consists of two climb dislocations with same magnitude of their Burgers vector but opposite direction and two glide dislocations with the same relation between their Burgers vectors. The dislocations are located at the end points of an element and the normal and shear stresses are calculated at the centre of the element.

The stress field from a dislocation in a Cartesian coordinate system situated at the origin is calculated from Eq. (1), cf. Hills *et al.* [13], where b_k are the Burgers vectors in the x and y direction and $G_{ij}^{k}(x,y)$ are the influence functions governing the stresses at point (x,y).

$$\sigma_{ij}(x,y) = \frac{2\mu}{\pi(\kappa+1)} \sum_{k=x,y} G_{ij}^{k}(x,y) b_k, \; i,j = x,y \tag{1}$$

The stress at an arbitrary point is calculated as the sum of the stress contribution from the external load and the stresses due the dislocations along the external boundary and eventual nucleated dislocations along the slip planes. The magnitude of the Burgers vector for the dislocations along the external boundary must be determined before the stress at an arbitrary point can be calculated. The normal and shear stresses along the external boundary must equal zero if the crack is open, which leads to an equilibrium equation from which the magnitudes of the Burgers vectors for the dislocations along the external boundary are determined. If parts of the crack are closed, the magnitude of the corresponding Burgers vector is put to zero.

The resolved shear stress τ_{slip} is calculated at all possible nucleation sites and a dislocation pair is assumed to nucleate if τ_{slip} exceeds the nucleation stress τ_{nuc}. This leads to a condition for nucleation according to Eq. (2) where θ is the angle between the global x-axis and the slip plane, and σ_{xx}, σ_{yy} and σ_{xy} the stresses at the nucleation point in focus.

$$\tau_{slip}(\theta) = \frac{\sigma_{yy} - \sigma_{xx}}{2} \sin 2\theta + \sigma_{xy} \cos 2\theta \geq \tau_{nuc} \tag{2}$$

Crack growth by emission and annihilation of discrete dislocations

Equation (1), giving the stress field from one dislocation, is not valid within the core radius of a dislocation, typically 1-5 Burgers vectors [11], and therefore the resolved shear stress by choice is calculated a distance of 6 Burgers vectors away from the crack. Because the complex geometry of the crack the nucleation stress must be recalculated at the beginning

of each new load cycle. The nucleation stress is defined as the stress at the nucleation point when the nucleated positive dislocation travels inwards in the material along the specific slip plane and the negative dislocation travels to the crack surface. The choice of nucleation stress is described in detail by Hansson and Melin [14].

At the beginning of the first loading cycle it is assumed that no dislocations within the material exist. During the loading part of the first cycle dislocation pairs will nucleate and form a plastic zone when the external load gets sufficiently high. The positive dislocations move along their respective slip plane as illustrated in Fig. 2.1. The negative dislocations are situated at the crack surface causing either a slip between the crack surfaces or the crack to open, depending from which slip plane it emanates. For every new dislocation pair nucleated, the shielding effect on the crack increases and the external load must be increased in order to nucleate further dislocation pairs. When the maximum load is reached, the load is reversed and the positive dislocations start to move closer to the crack if τ_{crit} is reached in the reverse direction, illustrated in Fig. 2.2. When a positive dislocation reaches the crack surface it annihilates and the crack advances one Burgers vector along the corresponding slip direction. This growth process through annihilation continuous until minimum load is reached and the next load cycle starts. If the crack has formed a kink a new slip plane is activated at the position of the new crack tip as illustrated in Fig. 1.

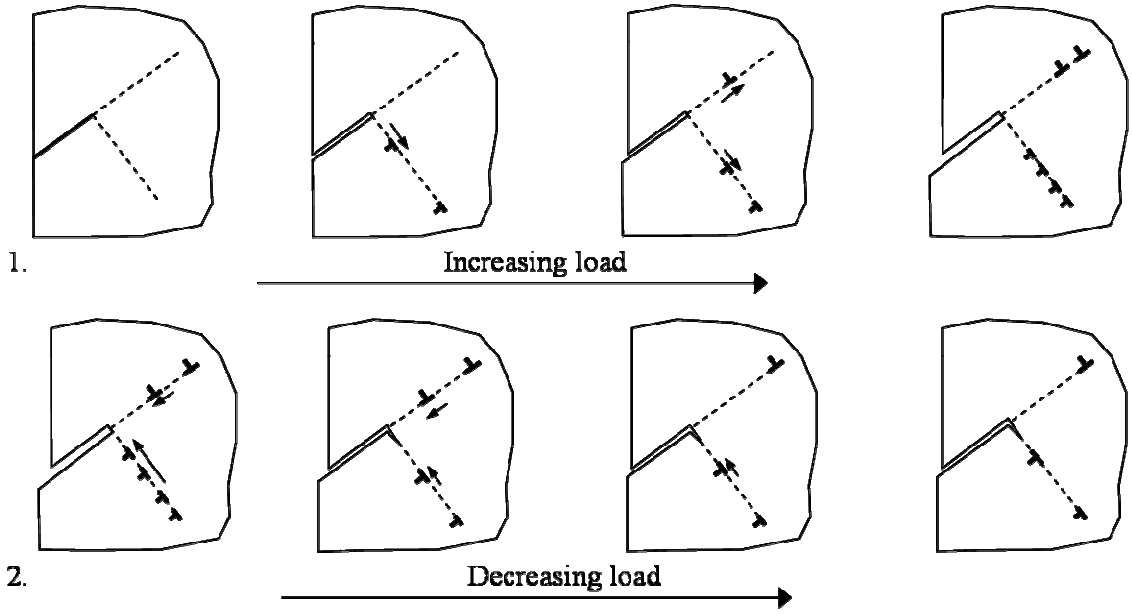

FIGURE 2. Schematic description of the first loading cycle during: 1. loading, 2. unloading. Only positive dislocations are shown.

Numerical implementation

The equilibrium positions of all positive dislocations, located along the different activated slip planes and forming the plastic zone, are found iteratively, cf. [8]. It is assumed that a dislocation moves a certain distance Δr along its slip plane if the resolved shear stress exceeds the critical resolved shear stress. Δr is calculated from Eq. (3), where C is a constant determining the movement of the dislocation. If C is too large the equilibrium location of the dislocations might not be found and if to low, the iterative process becomes uneconomical. At every load increment the equilibrium positions for the dislocations are found by this process and the resolved shear stress at all possible nucleation sites is compared to the nucleation

stress. The load is not allowed to increase until no further dislocation pairs are nucleated and the equilibrium positions for the positive dislocations are found.

$$\Delta r = C \frac{\tau_{slip} - \tau_{crit}}{\tau_{crit}} \tag{3}$$

Results

In this study the initial crack length is a_0 = 2.5 μm and the distance to the grain boundary from the original crack tip position is 1.25 μm. From a previous study of the same geometry, with the external load varying between $\sigma^{\infty}_{yy\,max}$ = 200 MPa and $\sigma^{\infty}_{yy\,min}$ = 0, five different crack patterns for crack growth within one grain could be observed [14], cf. Fig. 3. All five crack path patterns were present in the case of β = 70.6°, but only two, corresponding to numbers 3.4 and 3.5 in Fig. 3, in the case of β = 109.4°. In order to provoke the missing three crack paths 3.1-3.3 in Fig. 3 for β = 109.4°, the maximum load is increased in this study, whereas still the minimum load is $\sigma^{\infty}_{yy\,min}$ = 0.

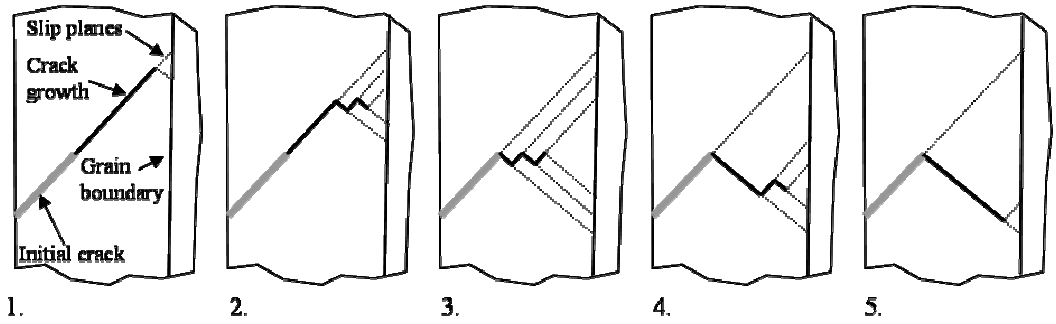

FIGURE 3. Crack growth patterns.

For the first two crack paths, Figs. 3.1 and 3.2, the crack grows along the initial slip plane, with the difference that the crack in Fig 3.2 eventually starts to grow in a zigzag pattern. The crack in Fig 3.3 starts to grow along the lower slip plane but immediately forms a zigzag shape. In Fig. 4 the crack shapes after a number of cycles for two different initial crack angels α are shown. All measures are in Burgers vectors with a_0 = 2.5 μm = 10000*b*. In Fig. 4.1, the initial crack angle α = 60° and the figure shows the shape after 10 load cycles. The crack path is in this case of the type in Fig. 3.3. For a larger initial crack angle, the crack initially grows along the upper slip plane. In Fig. 4.2 the initial crack angle α = 70°. The first part of the crack path, when the crack only grows along the upper slip plane, lasts for around 600 cycles where after the zigzag part is created during 10 cycles only**.**

At increasing value of α, eventually a situation at which the crack is prevented from growing is reached. This is due to the low resolved shear stress along the slip planes emanating from the crack tip at large angles α. In order to provoke the crack path in Fig. 3.1, no dislocations are allowed to nucleate along the lower slip plane because they will eventually be annihilated as the crack approaches the grain boundary, resulting in a change of crack growth direction and a crack path as in Fig. 3.2 would result. If the crack is growing, due to the high value of β, β = 109.4°, some dislocations will always eventually nucleate along the lower slip plane, independent of choice of α. Therefore the crack path in Fig. 3.1 can never be obtained, irrespective of choice of α and maximum value of external load.

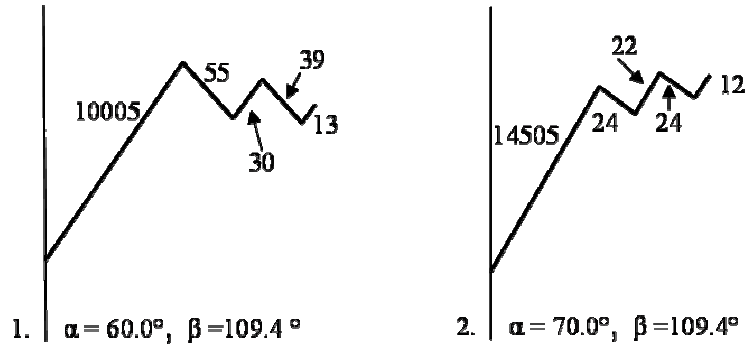

FIGURE 4. Crack shapes. All lengths are expressed in Burgers vector and the figures are not drawn to scale. The initial crack length a_0 = 2.5 μm = 10000*b*.

The crack growth rate, *da/dN*, where *a* is the crack length and *N* the number of cycles, for the cases in Fig. 4 are shown in Fig. 5 versus $\sqrt{a}$. In Figs. 5.1 and 5.2 α = 70° and corresponds to the crack path in Fig. 4.2. The growth rate increases as the crack gets longer while growing along the upper slip plane. When entering the zigzag part of the crack path, the growth rates changes dramatically between the different cycles. Similar behaviour is seen in the case of α = 60°, cf. Fig. 4.1 and Fig. 5.3. The decreases in growth rates in Figs. 5.2 and 5.3 are obtained in the cycles just before the crack is about to change its growth direction. The highest values correspond to the loading cycles just after the crack has changed its growth direction.

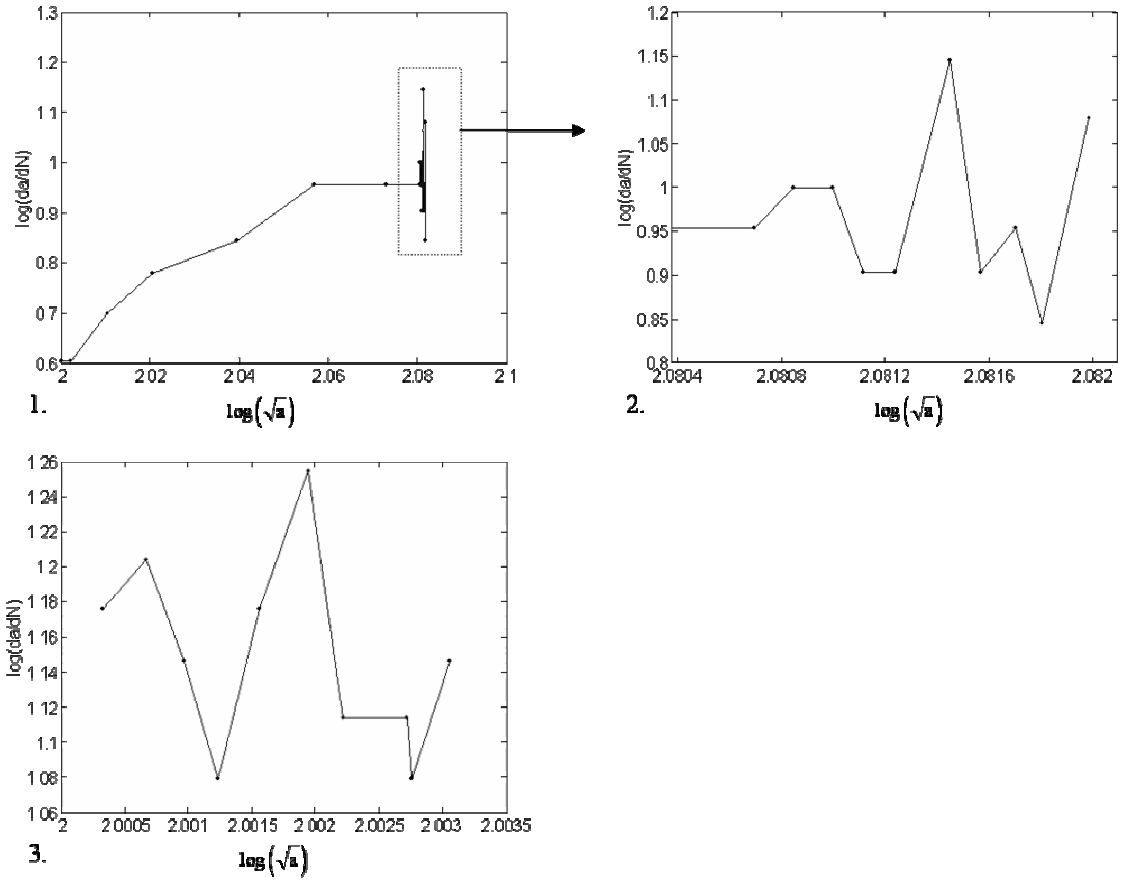

FIGURE 5. Crack growth rates as functions of crack length. Crack length and crack growth rates expressed in terms of Burgers vector, *b*.

The calculations also make it possible to monitor the development of the plastic zone, i.e. the dislocation distribution, during the cycles. In Fig. 6, the dislocation distributions during the 10th cycle at three different load levels for the case of initial crack angle α = 60°, Fig. 4.1, are shown. The dislocations have different markings depending on at which slip plane they are situated according to Fig. 6.3. At maximum load, in this case $\sigma^{\infty}_{yy\,max}$ = 280 MPa, a large number of dislocations are positioned along four different slip planes, cf. Fig. 6.1. When the load is decreased the dislocations move closer to the crack and some of them will eventually get annihilated at the crack surfaces. In Fig. 6.2 the external load is 40 MPa and 9 dislocations have been annihilated from the upper slip plane emanating from the crack tip, and it is clearly seen that the dislocations are more spread out over the slip planes. At minimum load, cf. Fig. 6.3, all dislocations along the upper slip plane and 1 dislocation from the lower slip plane emanating from the crack tip have been annihilated. The crack consequently grows a distance of 13 Burgers vectors in the direction of the upper slip plane and 1 Burgers vector along the lower slip plane, resulting in a new crack path direction in the cycle to follow.

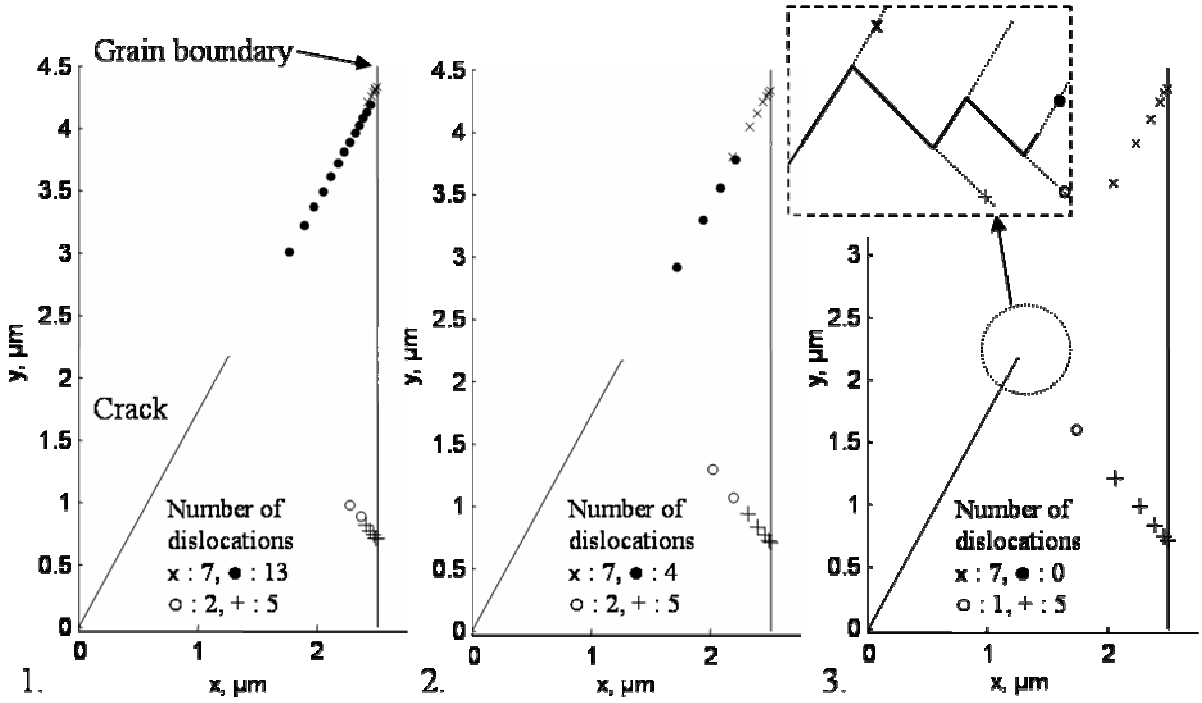

FIGURE 6. Dislocation distribution during the 10th cycle at external load equal to: 1. 280 MPa, 2. 40 MPa, 3. 0 MPa

Conclusions

Growth of a short edge crack within one grain of bcc iron subjected to fatigue loading has been modelled using a dislocation technique.

The formulation used in this study makes it possible to quantify zigzag crack paths emerging at crack growth through single shear. The development of the plastic zone can be studied in detail over the load cycles. It was found that it is the initial crack angle that determines the resulting crack path for a specific slip system subjected to fatigue loading. It was also found that change of the crack growth direction always resulted at growth in the slip system with angle between the slip planes β = 109.4°.

From the crack growth rate curves it was seen that the growth rate changes dramatically between different cycles during the zigzag formation of the crack path, whereas the curves are smooth as long as the crack extends straight forward. A general observation is that the growth rate decreases just before the crack changes its growth direction and that the growth rate is high in the cycles following directly after a change in growth direction

References

1. Paris, P. C., Gomez, M. and Andersson, E. E., *Thend Eng.* Vol. 13, 1961, pp. 9-14.
2. Suresh, S. *Fatigue of Materials, second edition*. University Press, Cambridge, 1998.
3. Andersson, H. and Persson, C. In-situ SEM study of Fatigue behaviour in IN718. Int Jnl of Fatigue 2004:26(6):211-219.
4. Jono, M., Sugeta, A. and Uematsu, Y. Atomic force microscopy and the mechanism of fatigue crack growth. Fatigue Fract Engng Mater struct 24, 831-842.
5. Zhang, J. Z., a shear band decohesion model for small fatigue crack growth in an ultra-fine grain aluminium alloy. Engineering Fracture Mechanics 2000:65:665-681
6. Riemelmoser, F.O., Pippan, R. and Stüve, H.P. An argument for a cycle-by-cycle propagation of fatigue cracks at small stress intensity ranges. Acta Mater. Vol. 46, No 5. pp. 1793-1799, 1998.
7. Riemelmoser, F.O. and Pippan, R. Mechanical reasons for plasticity-induced crack closure under plane strain conditions. Fatigue & Fracture of Engineering Materials & Structures 1998; **21**: 1425-1433.
8. Bjerkén, C. and Melin, S. A tool to model short crack fatigue growth using a discrete dislocation formulation. Int Jnl of Fatigue 2003:25(6):559-566.
9. Bjerkén, C. and Melin, S. Influence of grain boundary orientation on fatigue growth of a short crack in the vicinity of a grain boundary. ICM 9, Geneva, May 25-29, 2003.
10. Uematsu, Y., Sugeta, A., Motoyashiki, Y. and Jono, M. Analysis of fatigue crack deflection behaviour by means of discrete dislocation method. ICM 9, Geneva, May 25-29, 2003.
11. Hull, D. and Bacon, D, J. Introduction to Dislocations, fourth edition. Butterworth-Heinemann 2001.
12. D.R Askeland. The Science and Engineering of Materials, third edition. Stanley Thornes (Publishers) Ltd, 1998.
13. D.A. Hills, P.A. Kelly, D.N. Dai and A.M. Korsunsky. Solution of Crack problems: The distributed dislocation technique. Kluwer Academic Publisher, 1996.
14. Hansson, H. and Melin S. Dislocation modelling of crack growth through single shear due to fatigue loading of a short crack. To be published in *Int. J. Fatigue.*